Research Article
Turkish Journal of Maritime and Marine Sciences Volume: 3 Issue: 2 (2017) 113-120

Some Remarks on the Three Dimensionality of Hydrofoil Cavitation

Üç Boyutlu Hidrofoil Kavitasyonu ile İlgili Bazı Sonuçlar

Türk Denizcilik ve Deniz Bilimleri Dergisi Cilt: 3 Sayı: 2 (2017) 113-120

Mehmet Salih KARAALİOĞLU[1,2]*, Şakir BAL[1]

[1] *Department of Naval Architecture and Marine Engineering, Istanbul Technical University, Turkey*

[2] *Department of Naval Architecture and Marine Engineering, Ordu University, Turkey*

ABSTRACT

As it is well-known that cavitation is a very important physical phenomenon that affects significantly the performance of three-dimensional hydrofoils. Prediction of cavitation on three-dimensional hydrofoils is very important in the design stage. In this study, some approaches have been verified for hydrofoil cavitation. The main aim of this paper is to compare the mid-section pressure distribution of three-dimensional cavitating rectangular hydrofoil for increasing aspect ratios, with the pressure distribution of two-dimensional cavitating hydrofoil having the same section geometry as in the three-dimensional hydrofoil.

In this study, a boundary element (panel) method (BEM) has been applied to investigate the hydrofoil cavitation for both two- and three-dimensional cases. Two-dimensional analytical solution in case of cavitating flat-plate has also been applied for comparison. It has been shown that the pressure distributions on the mid-section of three-dimensional cavitating and non-cavitating hydrofoil for increasing aspect ratios have converged to the solutions in two-dimensional case

Keywords: Cavitation, boundary element method, hydrofoil, flat plate, aspect ratio.

Article Info
Received: 18 October 2017
Revised: 4 December 2017
Accepted: 8 December 2017

* (corresponding author)
E-mail: karaalioglum@itu.edu.tr

ÖZET

Bilindiği üzere, kavitasyon üç boyutlu hidrofoillerin performansını etkileyen çok önemli fiziksel bir olgudur. Dizayn açısından, kavitasyonun doğru hesabı önem arz etmektedir. Bu çalışmada, kavitasyon açısından yapılan bazı yaklaşımların doğrulanması yapılmıştır. Temelde yapılan çalışmanın amacı, üç boyutlu dikdörtgen bir kanadın ortasındaki ince bir dilim incelenerek iki boyutlu kesit ile üç boyutlu kanat arasındaki ilişkinin (basnç dağılımı cinsinden) artan yan oran ile incelenmesidir. Çalışmada kavitasyonlu iki ve üç boyutlu hidrofoillerin incelenmesinde sınır elemanları yöntemi kullanılmıştır. İki boyutlu hesaplamaların anlatıldığı bölümde, düz plaka için literatürde bulunan analitik çözümler de kullanılmıştır. Üç boyutlu durumun incelendiği bölümde, kanada ait orta kesitteki basınç dağılımının artan yan oran ile iki boyutlu değerlere yakınsadığı gösterilmiştir. Bu, hem kavitasyonlu hem de kavitasyonsuz durumda yapılmıştır.

Anahtar sözcükler: Kavitasyon, sınır elemanları yöntemi, hidrofoil, düz levha, yan oran.

1. INTRODUCTION

Cavitation occurs on the blades of hydrofoils, marine propellers, marine current turbines, and pumps and is a very critical problem in the design stages of these marine devices. Its prediction has gained an increasing importance in recent years and played a vital role in reducing undesirable effects of cavitation vibration, noise and material erosion. A number of techniques have been developed to estimate cavitation phenomenon for two- and three-dimensional hydrofoil problems such as boundary element methods, computational fluid dynamics, and experimental method. The boundary element method (BEM) is an efficient, robust and fast technique. In this study, a potential based boundary element method has been applied to two-dimensional and three-dimensional cases (Kinnas and Fine, 1993).

In the past, linear theory was used to formulate two dimensional cavitating hydrofoil flows by Tulin, Acosta and Geurst and Timman (Tulin, 1964; Uhlman, 1987). Linear theory was quite similar to classical thin wing theory. It was assumed that cavity and foil thickness relative to the foil chord length is thin (Kinnas, 1999). In the linear theory, when the foil thickness has been increased, the cavity volume and cavity size have been increased. This was not correct and contrary to the experimental results. Later, numerical nonlinear surface vorticity method was developed by Uhlman [3], contrary to linear theory, when the foil thickness has been increased, the cavity volume and size decreased , that is parallel to observations. Two dimensional hydrofoil was analyzed by using bucket diagram in terms of partial cavitation and cavitation inception (Karaalioğlu, 2015; Karaalioğlu and Bal, 2015).

The relationship between Circulation distribution on blade and cavitation and lift-drag coefficients has been investigated systematically (Karaalioğlu and Bal, 2016).

Horizontal axis marine turbine model was tested in cavitation tunnel and then blades of model turbine were modelled numerically using vortex lattice method by Bal *et al*. (2015). The comparison between simulation results and experimental data showed a slight difference in terms of span-wise extent of the cavitation region (Bal *et al*., 2015).

Occurrence of cavitation on horizontal axis marine current turbine blades has been investigated by Deniz and Bal using blade element momentum theory and boundary element methods (Uşar, 2015; Uşar and Bal, 2015).

Cavitating flows in three dimensions (three dimensional hydrofoils) have also been investigated by Nishiyama (1970), Furuya

(1975), Uhlman (1987). In these methods, three dimensional effects have been introduced by matching the inner solution with the solution from lifting line theory in the outer domain. However, these methods could also be applied only for hydrofoils with high-aspect ratios.

Celik *et al.* (2014) developed a new method for the prediction of cavity on two-dimensional (2D) and three-dimensional (3D) hydrofoils by a potential-based BEM. The results obtained by new method have been compared with those of other boundary element codes and a commercial CFD code (FLUENT) (Çelik *et al*., 2014). Bal *et al.* (2001) developed a model to describe 2D and 3D cavitating hydrofoils moving with constant speed under a free surface. This method was carried out for 2-D and 3-D hydrofoil geometries in fully wetted or cavitating flow conditions and obtained results are compared with those of other methods in the literature (Bal *et al*., 2001).

In this study, the mid-section pressure distribution of three-dimensional cavitating rectangular hydrofoil for increasing aspect ratios has been compared with the pressure distribution of two-dimensional cavitating hydrofoil having the same section geometry. Some remarks on hydrofoil cavitation has been made and the results have been validated with those of analytical ones.

2. MATHEMATICAL FORMULATION

The formulation of the problem has been given in Kinnas and Fine (1993) and Bal and Kinnas (2003) in detail. However, a brief summary of the formulation is given for the completeness of the study in this section. It is assumed that the flow around the hydrofoil is incompressible, inviscid and irrotational as shown in Figure 1. The steady flow can be defined in terms of total potential and perturbation potential functions.

$$\Phi(x,y,z) = \phi(x,y,z) + U_\infty x \tag{1}$$

Total potential and perturbation potential must be satisfied Laplace's equation.

$$\nabla^2\phi = \nabla^2\Phi = 0 \tag{2}$$

The following boundary conditions should also be satisfied on the surfaces of the problem.

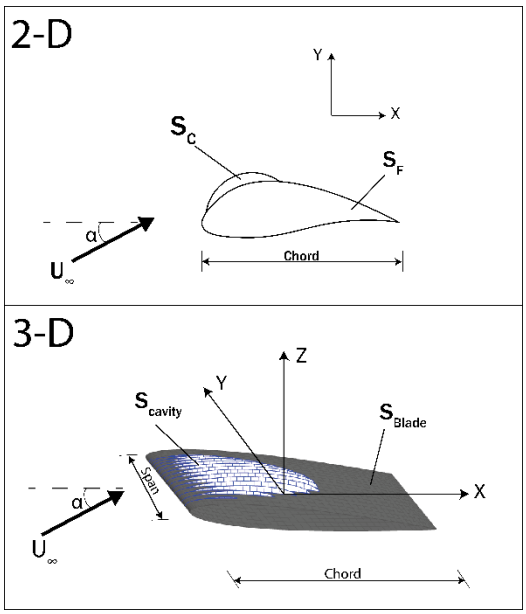

Figure 1. Definition of coordinate system for two- and three- dimensional case.

I. Kinematic Boundary Condition: The tangential component of velocity both on hydrofoil surface and cavity surface must be equal to zero. Velocity on cavity surface can be obtained by using Bernoulli equation (Bal and Kinnas, 2003).

$$\frac{\partial\phi}{\partial n} = -\frac{\partial\Phi_{in}}{\partial n} = U_\infty \vec{n} \tag{3}$$

II. Dynamic Boundary Condition: Pressure on the cavity surface is constant and equal to vaporization pressure.

$$q_c = U_\infty(1+\sigma)^{1/2} \tag{4}$$

where σ is cavitation number.

$$\sigma = \frac{p_\infty - p_v}{\frac{1}{2}\rho U_\infty^2} \tag{5}$$

III. Kutta Condition: The velocity in the trailing edge of the hydrofoil must be finite.

$$\nabla\Phi = finite \qquad \text{(Trailing edge.)} \qquad (6)$$

IV. Cavity Closure Condition: The trailing edge of cavity has complicated physical phenomena. A termination model must be applied at trailing edge of cavity to simplify the problem. Some termination models have been defined such as the pressure recovery model, the re-entrant jet model, the spiral vortex model, the viscous wake model. Pressure recovery termination model in has been applied in this study (Bal and Kinnas, 2003).

Mathematical formulation for three-dimensional case is similar to that of two-dimensional case. Above boundary conditions are also valid for three-dimensional case. In addition, third component of coordinate system should be included into formulations (Bal, 2011).

3. NUMERICAL IMPLEMENTATION

3.1. 2-D Problem

By applying Green's third identity, the perturbation potential at p can be expressed as;

$$2\pi\phi_p = \int_S \left[-\phi \frac{\partial \log R}{\partial n} + \frac{\partial \phi}{\partial n} \log R \right] dS$$

$$-\int_W \Delta\phi_w \frac{\partial \log R}{\partial n} dS \quad \text{for p outside S and W} \qquad (7)$$

$$\pi\phi_p = \int_S \left[-\phi \frac{\partial \log R}{\partial n} + \frac{\partial \phi}{\partial n} \log R \right] dS$$

$$-\int_W \Delta\phi_w \frac{\partial \log R}{\partial n} dS \quad \text{for p on S and W} \qquad (8)$$

where R is distance from the surface element dS to the point, W is the surface of wake and S is the surface of the wetted foil or cavity.

Perturbation potential can be represented in terms of dipole distribution of the strength ϕ, source distribution strength $\partial\phi/\partial n$, and dipole distribution of constant strength $\Delta\phi_w$

Cavity and foil surface can be discretize into straight panels whose vertices lie on S in order to invert numerically Equation 8.

The cavity surface is not known and is obtained iteratively. At first iteration the cavity panels are putted on the foil underneath it. At each iteration the edges of the cavity of the cavity panels are relocated on the current cavity surface which was computed at the end of previous iteration (Kinnas and Fine, 1990).

3.2. 3-D Problem

The integral equation can be obtained by applying the Green's third identity to the governing equation in the fluid domain for the perturbation potential on the cavity and wetted hydrofoil surfaces.

$$2\pi\phi_p = \iint_{S_{cavity+blade}} \left[\phi \frac{\partial}{\partial n}\frac{1}{R} - \frac{\partial \phi}{\partial n}\frac{1}{R} \right] dS + \iint_{S_{wake}} \left[\Delta\phi_w \frac{\partial}{\partial n}\frac{1}{R} \right] dS \qquad (9)$$

In present method, hydrofoil and cavity surface are discretized into quadrilateral panels. Constant-strength source and dipole panel on the foil and constant-strength dipole panels on the presumed wake surface is used. Equation 9 is carried out at control point of each panel by using a low order panel method iteratively. Strength of dipoles and sources are unknown.

Unknowns are found by solving linear system of equations. Then cavity thickness is obtained by integrating the source strength. The cavity volume history and the forces can then be computed by integrating the cavity thickness and the pressures, respectively.

The cavity shape is determined in fixed-cavitation number approach. In this method, the cavitation number is assumed to be known and the cavity length, shape and volume can then be determined. Cavity length and cavity shape is determined with an iterative method. The iteration procedure is repeated until both kinematic and dynamic boundary conditions are satisfied on the section surfaces of blades under the

cavity surface. The details of the method are given in Katz and Plotkin (2001).

4. NUMERICAL RESULTS

First, the analytical solutions for partial cavitating flat plate have been given below as described in Furuya (1975). Also the terms in the formulations of partially cavitating flat plate has been presented in Figure 2.
By defining the angle β from:

$$l = \cos^2 \beta \tag{10}$$

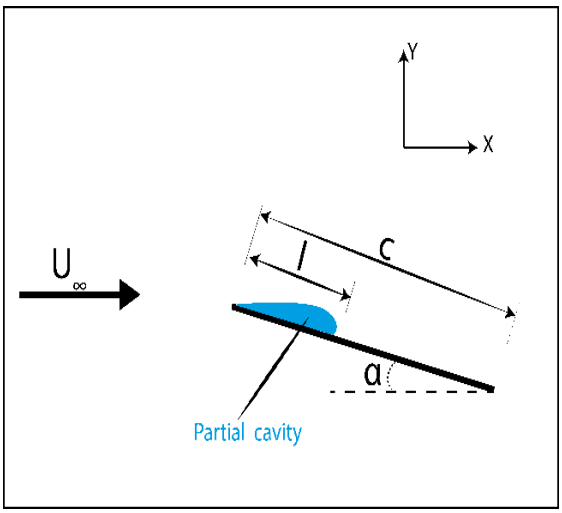

Figure 2. Partially cavitating plate.

$$\frac{\alpha}{\sigma} = \frac{1}{2}\tan\beta\frac{1-\sin\beta}{1+\sin\beta} \tag{11}$$

$$V = \frac{\pi\alpha}{16}\cot\beta(1+4\sin\beta-\sin^2\beta-4\sin^3\beta) \tag{12}$$

$$C_L = \pi\alpha\left(1+\frac{1}{\sin\beta}\right) \tag{13}$$

$$C_M = \frac{\pi\alpha}{8}(-3-6\sin\beta+\sin^2\beta+4\sin^3\beta) \tag{14}$$

$$C_D = \alpha C_L \tag{15}$$

where V is the cavity volume, C_L the lift coefficient, C_M the moment coefficient with respect to mid chord and C_D the cavity drag coefficient. Closed solution of flat plate is given in Figure 3. If closed solution scaled with the angle of attack, solution depends on only cavity length. For each α/σ, short and long cavity solution exist. But long cavity is unstable and physically unaccepted. So it is discarded here. Maximum of cavity length is ¾. Later numerical solution obtained by 3D BEM has been compared with this closed form (analytical) solution. To do this, a cavitating rectangular hydrofoil having NACA0002 sections along span direction, with aspect ratio (AR=8) has been chosen. The cavity lengths on the mid-section can therefore be compared with that of analytical solution. Figure 3 shows the ratio of angle of attack to cavitation number versus ratio of cavity length to chord length for cavitating mid-section of 3D rectangular blade as compared with the analytical solution. The blade have NACA0002 profiles along the spanwise direction and the aspect ratio (s/c) is 8. The differences between analytical and numerical solutions are small for small angles of attack (or for large cavitation numbers) as expected. For higher angles of attack (or small cavitation numbers) the effects of thickness ratio (here t_{max}/c=0.02) becomes important.
In 3D calculations, the numbers of panels in the x direction and y direction are chosen as 100 and 41 respectively for all cases. Total number of panels on blade is therefore 100*41=4100. Those number of panel have been reached by systematic numerical tests. Cosine spacing in x and y direction is used on the blade (Bal and Kinnas, 2003).

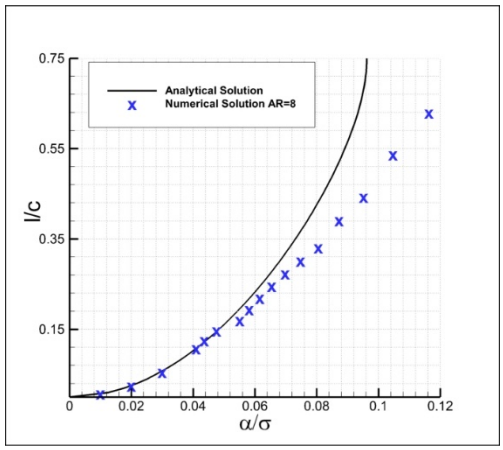

Figure 3. Comparison of analytical solution of cavitating flat-plate with numerical one (AR=8 Mid-section solution).

Later, for non-cavitating case, the blade section geometry of 3D hydrofoil is chosen as NACA0012 with angle of attack 5º. The non-dimensional pressure distributions on the mid-sections are shown for increasing aspect ratios as compared with that of 2D solution in Figure 4. The mid-section strip has, on the other hand, been shown in Figure 5. As the aspect ratio is increasing, the non-dimensional pressure distribution on the mid-section of 3D hydrofoil is converged to that of 2D section.

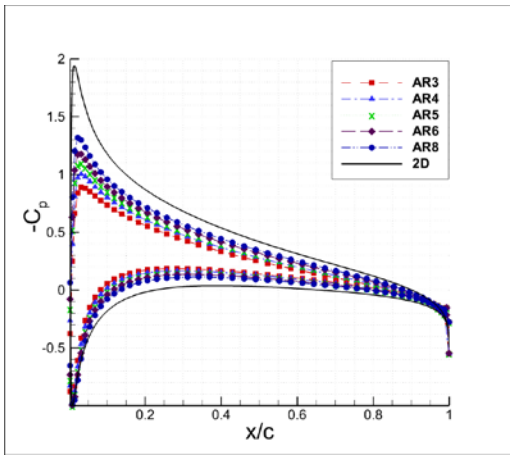

Figure 4. Comparison of non-dimensional pressure distributions on mid-sections of 3D hydrofoils with 2D solution, α=5º (Non-cavitating case).

For the cavity case, the calculations are then done for the 3D hydrofoil with the ratio of cavity length to chord length, l/c=0.5473. The hydrofoil has NACA0002 sections along span direction and the angle of attack has been chosen as three degrees. In Figure 5, the 3D view of cavity shape has been shown for cavitation number, σ=0.44.

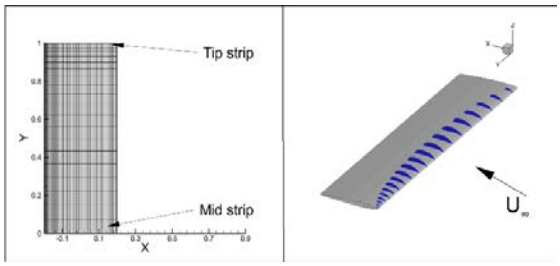

Figure 5. Panel distribution on half of blade (left) and cavity distribution on full blade with $\alpha=3^0$ for s/c=5.

In Figure 6, the cavity shapes on mid-section, with different aspect ratios have been compared with that of 2D solution. The non-dimensional pressure distribution (C_P) on the mid-section of 3D blade for different aspect ratios and two dimensional solution ($t_{max}/c=0.02$) has also been shown in Figure 7. Note that the sharp pressure decrease in termination of cavity surface is due to decreasing velocity values in Figure 7 and Figure 8.

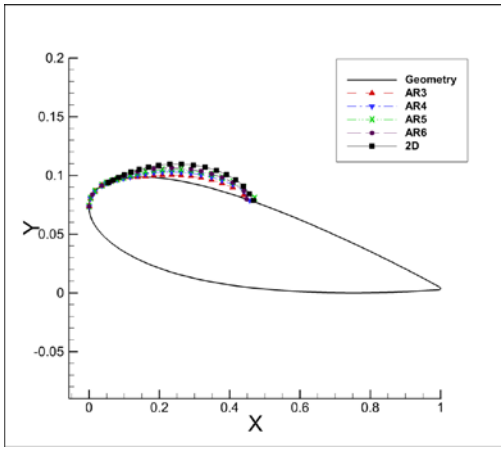

Figure 6. Comparison of cavity shape of mid-sections of 3D hydrofoils with 2D solution, α=4º σ_{2D}=0.75252.

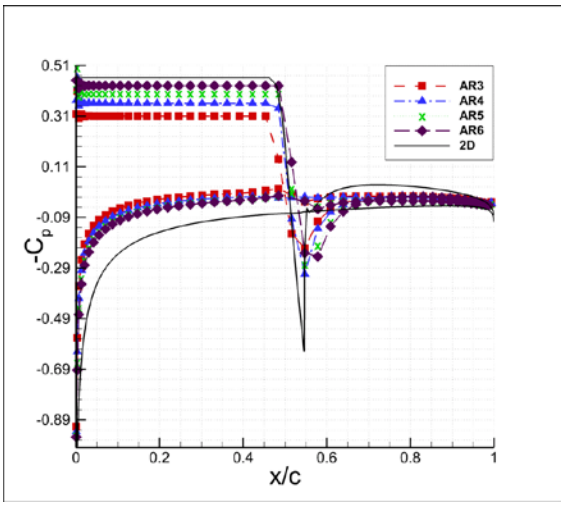

Figure 7. Pressure distribution on mid-section of blade and two dimensional section for l/c=0.5473, NACA0002, $\alpha=3^0$.

The calculations are done for cavity length to chord ratio (l/c=0.754) as well. The non-dimensional pressure distributions have been shown for this case in Figure 8. Note that increasing aspect ratios give closer results to two-dimensional solution as expected.

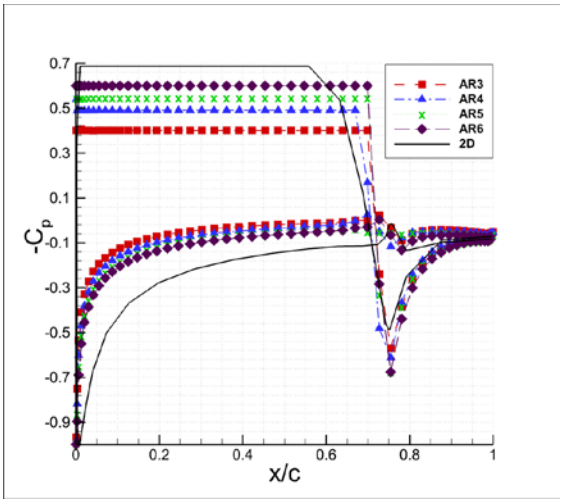

Figure 8. Pressure distribution on mid-section of blade and two dimensional section for l/c=0.7543 NACA0002, $\alpha=3^0$.

The effect of foil thickness on cavity surface has later been shown in Figure 9. All sections operate at angle of attack, $\alpha=2^0$ and cavitation number, $\sigma=0.651$. Note that cavity size decreases with increasing foil thickness.

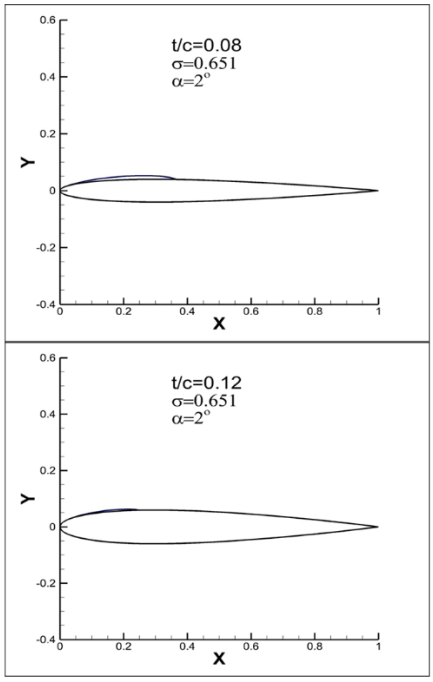

Figure 9. Cavity shape for different thickness ratio (2D $\sigma=0.651$, $\alpha=2^0$).

5. CONCLUSION

Two- and three-dimensional hydrofoil cavitation has been analyzed by using a perturbation potential based panel method. For three-dimensional case, the pressure distribution on the mid-section of cavitating and non-cavitating blades for increasing aspect ratios has been found to converge to the solution of two-dimensional problem. For three-dimensional case, the cavity shape on the mid-section of cavitating 3D blades for increasing aspect ratios has also been found to converge to the solution of two-dimensional problem.

Nomenclature

AR = Aspect Ratio [s/c]
2D = Two-dimensional
3D = Three-dimensional
α = Angle of attack
V = Cavity volume
L = Lift
D = Drag
ρ = Density
σ = Cavitation number

C_D = Drag coefficient [$\frac{2D}{c\rho U_\infty^2}$]

C_L = Lift coefficient [$\frac{2L}{c\rho U_\infty^2}$]

C_M = Moment coefficient

C_p = Pressure coefficient [$\frac{p_m - p_\infty}{0.5\rho U_\infty^2}$]

U_∞ = Inflow velocity

ϕ =Perturbation potential

p_∞ = Total pressure

p_v= Vaporization pressure

p_m= Static pressure

n = unit vector normal to the foil surface and cavity surface.

l = Cavity length

s = Span length

c = Chord length

t_{max} = Maximum thickness ratio of hydrofoil

S_c = Cavity surface

S_f = Foil surface

W, S_w = Wake surface

R = Distance from surface element

Φ = Total potential

6. REFERENCES

Kinnas, S. A., Fine, N. E. (1993). MIT-PCPAN and MIT-SCPAN (Partially cavitating and super cavitating 2-D panel methods) User's Manual, Version 1.0.

Tulin, M. P., (1964). Supercavitating Flows Small Perturbation Theory, J. Ship Res. 7: 16–37.

Uhlman, J. S., (1987). The Surface Singularity Method Applied to Partially Cavitating Hydrofoils, J. Sh. Res. 31 (2): 107–124.

Kinnas, S. A. (1999). Fundamentals of Cavity Flows, Austin.

Karaalioğlu, M. S. (2015). Hidrofoillerin Kavitasyon Kovalarının Sayısal-Parametrik İncelenmesi, İstanbul Teknik Üniversitesi, Fen Bilimleri Enstitüsü, İstanbul.

Karaalioğlu, M. S., Bal, Ş., (2015). Numerical Investigation Cavitation Buckets for Hydrofoil Parametrically, Turkish Journal of Maritime and Marine Sciences 1(2): 89-101.

Karaalioğlu, M. S., Bal, Ş., 2016. Investigation of hydrodynamic performance of cavitating blades of marine current turbines in uniform flow, 1St International Congress on Ship and Marine Technology.

Bal, Ş., Atlar, M., Usar, D., (2015). Performance prediction of horizontal axis marine current turbines, *Ocean Syst. Eng.* 5(2): 125–138.

Uşar, D. (2015). Sualtı Akıntı Türbinlerinin Hidrodinamik Analizi, Doktora Tezi, İstanbul Teknik Üniversitesi.

Uşar, D., Bal, Ş., (2015). Cavitation simulation on horizontal axis marine current turbines, *Renew. Energy*, 80: 15–25.

Nishiyama, T. (1970). Lifting-line Theory of Supercavitating Hydrofoil of Finite Span, *ZAMM - Zeitschrift für Angew. Math. und Mech.* 50(11): 645–653.

Furuya, O., (1975). Nonlinear calculation of arbitrarily shaped supercavitating hydrofoils near a free surface, *J. Fluid Mech.* 68 (1): 21.

Celik, F., Arikan Ozden, Y., Bal, S., (2014). Numerical simulation of flow around two- and three-dimensional partially cavitating hydrofoils, *Ocean Eng.* 78: 22–34.

Bal, S., Kinnas, S. A., Lee, H., (2001). Numerical Analysis of 2-D and 3-D Cavitating Hydrofoils under a Free Surface, *J. Sh. Res.* 45(1): 34–49.

Kinnas, S. A., Fine, N. E., (1993). A numerical nonlinear analysis of the flow around two- and three-dimensional partially cavitating hydrofoils, *Journal of Fluid Mechanics* 254(1):151.

Bal, S., Kinnas, S. A., (2003). A numerical wave tank model for cavitating hydrofoils, *Comput. Mech.* 32 (4–6): 259–268.

Bal, S., (2011). The effect of finite depth on 2D and 3D cavitating hydrofoils, *J. Mar. Sci. Technol.* 16(2): 129–142.

Kinnas, S. A., Fine, N. E. 1990. Non-linear Analysis of Flow Around Partially or Super-Cavitating Hydrofoils by a Potential Based Panel, Proceeding the IABEM-90 Symposium.

Katz, J., Plotkin, A. (2001). *Low-Speed Aerodynamics*. Cambridge University Press.